Seasonality Effects over the Classification Model using Machine Learning to Distinguish Natural from Anthropic Oil Slicks

Gil Marcio Avelino Silva*[1], Fernando Pellon de Miranda[1], Ítalo de Oliveira Matias[2], Patrícia Carneiro Genovez[2], Sarah Barrón Torres[2], Francisco Fábio de Araújo Ponte[2], Gustavo Araújo de Carvalho[3] [1]CENPES/Petrobras, [2]LES/PUC-Rio, [3] COPPE/UFRJ

This paper was prepared for presentation during the 17th International Congress of the Brazilian Geophysical Society held in Rio de Janeiro, Brazil, 16-19 August 2021.

Abstract

Distinguishing between natural and anthropic oil slicks is considered a challenging task, especially in Gulf of Mexico where these events can be simultaneously observed and recognized as seeps or spills. In this context, the powerful data analysis provided by Machine Learning (ML) methods was employed to develop, test, and implement a classification model (CM) to distinguish the oil slick source (OSS). From a database containing 4,916 oil samples, detected using Synthetic Aperture Radar (SAR), there were 408 spectral and 10 geometric features. The exploratory data analysis successfully reduced the dataset without compromising the model accuracy, selecting 12 features for the CM designing. An innovative approach evaluated how external factors like seasonality limit or improve the OSS predictions. To accomplish this, specific classification models (SCM) were derived from the global, tuning the best algorithms and parameters according to different scenarios. The median accuracies results revealed winter and spring as the best seasons. Among the six tested ML algorithms, Random Forest (RF) was the most robust, performing better in more than half of the investigated scenarios. The global CM achieved 73.15% of maximum accuracy using RF. The accuracy increment provided by the well-fitted models may minimize the confusion between seeps and spills. This represents a concrete contribution to reduce economic and geologic risks derived from exploration activities in offshore areas. Additionally, from the operational standpoint, specific models support specialists to select the best seasons for new acquisitions, as well as to optimize performances according to available data.

Introduction

The imminent risk of environmental, social, and economic impacts caused by oil pollution highlights the importance of identifying the source of the slicks. The oil spill detection may assist environmental regulatory agencies in the application of legal sanctions, as well as support the clean-up operations during emergency response actions [1],[2]. On the other hand, oil seep identification protects the oil industry against penalties for events in which there was no human interference. Additionally, the geologic risks related to the discovery of new exploration frontiers may be minimized [3].

Synthetic Aperture Radars (SAR) are the main instrument used for detecting and monitoring mineral oil slicks operationally. These remote sensors have potential to provide data in near real-time, during the day and night, under all weather conditions, combining different bands, resolutions, incidence angles and polarizations [1],[2],[4].

Regardless of whether the source is natural or anthropic, mineral oil slicks induce the same physical mechanism of damping the sea surface roughness. Consequently, these events are similarly detected as dark spots regions with low backscatter response in SAR images [5],[6], making the pollution source identification defiant. Several factors significantly affect the oil slick detection [9], including: (i) type and volume of oil; (ii) SAR antenna configuration, image acquisition parameters, data format and pre-processing techniques; (iii) meteo-oceanographic conditions and presence of false alarms (FA), known as lookalikes.

Despite the backscattering similarities, different weathering processes may change the physicochemical properties of mineral oils and, consequently, their detectability in SAR data [2]. Moreover, the patterns observed in terms of shape, dimensions, persistence, and spatial recurrence are also distinct, adding important information when designing a classification model (CM) [4].

Considering as reference a large database collected and validated over 13 years [7-9], the proposed research aims to develop a CM to differentiate natural from anthropic oil slicks using these time series of calibrated RADARSAT-2 data. To accomplish this, several spectral, geometric, and ancillary features were used as predictive (independent) attributes to learn and recognize patterns related to the categorical (dependent) one, named as Oil Slick Source (OSS).

Machine Learning (ML) is widely indicated to deal with scientific problems like this, without a defined solution, but with a large and validated database to be statistically explored and learned [10]. ML algorithms are useful to integrate and extract knowledge from diverse features with different statistical properties, being able to recognize patterns and generalize models to predict simple and complex classes [10-12].

Developing a CM is a challenging task. To consolidate a reliable model is required not only to select the best set of

attributes, algorithms, and parameters but also to understand which conditions may limit or improve its performance. In this context, the present research offers a unique perspective, evaluating the effects of the seasonality on the proposed CM. As a result, a few specific classification models (SCM) were derived from the global.

The oil and gas industry increasingly demands scientific solutions at a multidisciplinary level, integrating data and methodologies to develop intelligent systems. This research reflects these tendencies and shows how ML represents an efficient way to extract knowledge and improve the CM accuracy to identify the OSS.

The Gulf of Mexico (GoM) is known for the high incidence of petroleum seepage mostly concentrated in deep-water offshore regions. The optimal conditions needed to cause oil seepage are present there, including the abundant oil and gas reservoirs, as well as geological faults that induce hydrocarbon migration from the seafloor up to the sea surface. Despite 95% of released oils in the GoM are of natural origin, man-made mineral oil slicks may simultaneously occur. These spills are derived from petroleum exploration, production, transportation, and consumption activities [3],[13].

Situated in the southern GoM, the study area comprises the offshore region of the Campeche Bay, where prolific oil and gas reservoirs are located. The Cantarell complex is an important production asset that was discovered in 1976 and until recently exploited as a monopoly by the state-owned PEMEX (Petróleos Mexicanos). The spatial and temporal recurrence of oil seeps in the Campeche Bay [13], particularly in Cantarell, consolidated this region as an important test site, offering the possibility to validate oil slick detection using SAR images.

Furthermore, the GoM presents a strong seasonal variability in terms of meteo-oceanographic conditions, remarkably for wind intensity, including extreme climatic events like tropical cyclones and hurricanes [14],[15]. The winds also drive the dynamic of water circulation, transporting waters with different temperature and salinity [15].

Theory and Method

Meteo-oceanographic conditions, such as intensity of winds and currents, wave height and sea surface temperature, have a direct effect over the sea surface roughness attenuation [4]. Generally, wind intensities ranging from 3 to 10 $m.s^{-1}$ are considered suitable for oil detection, producing enough contrast between the oil slicks and the surrounding ocean [5],[6]. Low winds (≤3 $m.s^{-1}$) attenuate the sea surface roughness producing backscattering coefficients similar to the oil-contaminated patches, while higher wind intensities (≥10 $m.s^{-1}$) fragment, disperse, and mix the oil into the ocean making the detection unfeasible [5].

Other natural phenomena like algae blooms, biogenic oils, upwelling cold water, and rain cells can be mistakenly detected as mineral oils in SAR sensors. It is important to highlight that the interference of lookalikes is not considered in this research.

There are different distortions generated by the SAR sensor inherent to the image acquisition process. The system can suffer many losses affecting the power density of the reflected signal detected by the antenna [16]. Therefore, the pre-processing images stage, that is, the SAR data calibration is essential to perform quantitative analysis using spectral and geometric properties extracted from time series of data, as proposed here.

There are three types of calibration, as follows: (i) Sigma (S: σ_0): projected signal on the Earth's surface (Ground-Range); (ii) Beta (B: β_0): backscattered signal in the inclined range (Slant-Range); (iii) Gamma (G: γ_0): backscattered signal on the incident wavefront (perpendicular to the Slant-Range) [16]. The calibrated power images can be converted to decibel (dB), using as formats amplitude (A) or intensity (I), where I is equal to A^2. Applying filtering to remove the speckle noise is another common data treatment.

Beyond the spectral properties, geometric attributes like area, perimeter, and derivate metrics can be extracted from the satellite imagery providing valuable information about oil slick dimensions. Even if knowing that oil seeps and spills may be confused because of their similar dimensions, attributes such as shape and compactness can reveal different associated patterns. The shape indicates how irregular and fragmented the edges of the oil slicks are, while the compactness reveals their roundness level. Oil slicks with larger dimensions may remain on the sea surface longer, suffering a higher fragmentation of the edges by the weathering processes, action of waves and currents. Particularly in Cantarell, where seepage slicks can be predominantly larger than the anthropic ones [9], geometric properties may improve the predictive potential of the CM.

During the last decades, a number of ML algorithms have been widely employed to solve a range of classification and regression problems using multiple sources of data, including remote sensing [11]. ML algorithms are useful in generalizing models to detect simple and complex classes. They are also effective for handling large datasets including input features of different types, formats, and statistical properties. The ML workflow involves recognizing patterns, memorizing, remembering, and adapting them automatically to build intelligent systems [17].

Discriminate the OSS is an example of a complex real-world application, that requires a higher data dimensionality because of the spectral similarities between seeps and spills. In these cases, it is almost humanly impossible to find redundancies, statistical dependence-relations, select attributes and recognize patterns without using computational methods. Therefore, supervised ML algorithms are powerful to extract knowledge employing different statistical approaches to learn from multiple dimensions automatically in a controlled way [17].

In the last 20 years, significant achievements have been reported regarding the contributions of ML to develop automatic and semi-automatic systems for oil slick detection at the sea surface [13], allowing to minimize the human subjectivity and to improve the prediction performance. According to the scientific community, there is no perfect ML algorithm [11]. The selection is challenging mainly because their performance is case-specific, being affected by many factors that can be listed, among others, as: quantity and quality of the remote sensing data; dataset dimension and statistical properties of the predictor features; number and complexity of the classes; training and test samples balancing [11],[12].

Furthermore, to consolidate a robust and operational classification model, it is necessary not only to select the best set of attributes, algorithms, and parameters, but also to understand which conditions may limit or improve its performance.

The starting point for the present research is the database compiled, reviewed, and described by Carvalho et al. [3], [7-9]. It includes 4,916 samples detected in 277 RADARSAT-2 images, being 2,021 oil seeps and 2,895 spills, all of them validated by PEMEX. The available dataset follows all recommended parameters for oil detection, gathering a long time-series of radar imagery acquired in C band, with VV polarization and covering the proper range of incidence angles.

The radar images were pre-processed and interpreted. The oil slick geometry was delineated by the Unsupervised Semivariogram Textural Classifier (USTC) [13]. From each oil slick, 418 predictive features were extracted, as follows: (a) 10 geometric: shape and dimensions; (b) 408 spectral: statistical measures comprising combinations of backscattering coefficients calibrated in Sigma (S: σ_0), Beta (B: β_0) and Gamma (G: γ_0), using amplitude (A) and decibel (dB) formats, as well as evaluating the benefits of the Frost (F) filter application for speckle noise reduction.

Figure 1 provides the database overview in terms of number and features type. A description about the complete database, indicating features calculation and applied transformations are available in Carvalho et al. [7-9].

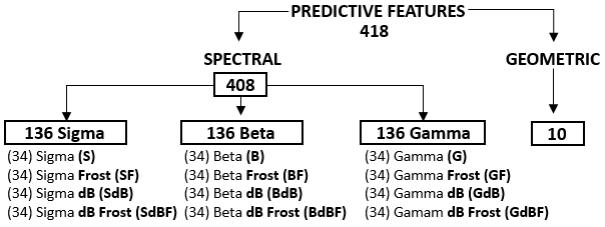

Figure 1 *– The number of geometric and spectral features (these ones per calibration, format, and speckle filtering).*

The dependent categorical feature, Oil Slick Source (OSS), assigns the class Seep (1) or Spill (0) for each sample and constitutes the key to the successful learning process.

The described dataset was used to carry out the predictive analysis and to develop a CM to distinguish the OSS. In order to understand the stability and the potential of the model, which should operate under different environmental conditions, an ancillary feature was added: seasonality. From the total oil slicks, 921 (18,73%) were detected in Winter, 1,660 (33,77%) in Spring, 1,130 (22,99%) in Summer and 1,205 (24,51%) in Fall.

Step I: To employ the exploratory data analysis (EDA) as part of the features pre-processing, for detecting and treating multiple correlations, outliers, missing values, spurious and redundant attributes, as well as for selecting an optimal subset. Different uni and multivariate statistical techniques were applied, such as: i) correlation matrices; ii) boxplots and histograms; iii) multi-dimensional scaling (MDS); iv) hierarchical clustering dendrogram using the Unweighted Pair Group Method with Arithmetic Mean (UPGMA). The MDS was used to group similar features as a basis to select the attributes and to reduce the dataset dimensionality. The correlation matrices, boxplots and dendrograms offered support for a supervised selection. At the end of the process, only one feature per MDS group was kept. This procedure was initially performed 12 times (one for each block of 34 spectral attributes; see Figure 1) and then once for the geometric ones, with the objective of selecting the best features.

Step II: To perform supervised classifications using as input the spectral and geometric features selected by the EDA. Six (6) well-known and consolidated ML algorithms were evaluated, as follows: (i) parametric: Gaussian Naïve Bayes (NB), Linear Discriminant Analysis (LDA) and Logistic Regression (LR); and (ii) nonparametric: Artificial Neural Networks (ANN), Random Forest (RF) and Decision Tree (DT). The global accuracies were used as a reference to select the best set of attributes, including the integration between geometric and spectral features, splitting 70% of the samples for training and 30% for testing.

Step III: To develop a global CM with sufficient generalization capacity, combining the best attributes, ML algorithms and parameters to discriminate the OSS. The set of parameters required by the algorithms affects the classification accuracies, especially for the nonparametric methods, which demand a higher number of parameters to be fitted.

Step IV: To design SCM using the global CM as a reference and considering the seasonality as ancillary data. The goal is to optimize the model to operate under different meteo-oceanographic conditions. As a result, 5 different scenarios were created to investigate the effects of the four seasons.

All steps of this methodology were carried out using Python. Furthermore, a software prototype was implemented making it possible to test and evaluate automatically all scenarios employing different ML algorithms.

Results

The EDA was conducted in two stages: the first focused on the spectral properties; the second evaluated the geometric features.

During the first stage, the correlation matrices show that the spectral features are multicorrelated, highlighting the need for a data dimensionality reduction. Then the MDS clustered each block of 34 features (Figure 1) into 5 distinct groups. The smaller the distances between the correlations, the greater the similarity between the features within the cluster, consolidating strategic blocks to perform the selection.

For all sets of 34 features, the MDS found three stable groups, such as: Group 1) Central tendency: Average (Avg), Median (Med), Mode (Mod) and Sliced Average (Mda); Group 2) Dispersion: Variance (Var), Standard Deviation (Std), Range Maximum - Minimum (Rng), Average Absolute Deviation (Aad), Median Absolute Deviation (Mad) and Coefficient of Dispersion (COD); Group 3) Coefficients of Variation (COV) with the Variance in the numerator: Var/Avg, Var/Med, Var/Mod and Var/Mda. The rest of attributes, with greater variability, was clustered into groups 4 and 5.

The redundancies were analyzed and only one attribute was selected per MDS group. In this process, the correlation matrices were used to map and exclude multicorrelated features with coefficients ≥ 0.9. The histograms per feature provided a comparison between the probability density functions, giving an idea about the separability between the classes of seeps and spills. The boxplots permitted to identify and select those attributes with lower overlapping between the statistical distributions. The dendrograms were analyzed to support the selection. Therefore, using an integrated approach, only five features remained per type of attribute.

Subsequently, considering as input the five features selected per attribute type, the supervised ML algorithms (ANN, RF, LDA, LR, NB and DT) were performed to evaluate the best calibration type, data format and filtering benefits.

Since the LDA returned the better performances, this algorithm was used as a reference to interpret the results below and recommend the proper calibration, data format, as well as the benefits of the filtering.

Calibration: the results (accuracies) were quite similar between S (68.54), B (69.29) and G (68.27), which is reasonable considering that S, B and G are trigonometric derivations of one another, showing similar behavior and strong multi-correlations. Sigma is recommended since it is widely used by the scientific community, representing the surface backscattering cross section, where the mechanisms for oil detection are prevalent.

Data format: the amplitude format returned relative better accuracies than dB for all calibrations S (A: 68.54; dB: 67.66), B (A: 69.29; dB: 67.59) and G (A: 68.27; dB: 65.42). Moreover, the image processing systems usually do not include the decibel format; this is another reason to extract the features using the amplitude format instead of dB.

Frost Filter: the filtering did not yield a significant contribution, instead reducing global accuracies. This was observed for all calibrations, as follows: Data in amplitude S (A: 68.54; AF: 64.34), B (A: 69.29; AF: 63.86), and G (A: 68.27; AF: 63.80); data in decibel S (dB: 67.66; dBF: 67.25), B (dB: 67.59; dBF 66.64), and G (dB: 65.42; dBF: 64.27).

Therefore, 408 spectral features were reduced to 34, keeping only the Sigma calibration in amplitude format without Frost filtering. These attributes could be reduced once more using the MDS clusters as a basis, eliminating the higher correlations and redundancies without damaging the predictions. At the end of the process, five **spectral features**, calibrated in Sigma and in amplitude format, were selected: **S_Avg, S_Rng, S_CodAvg, S_VarAvg and S_StdMed.**

The same EDA was performed to select the best **geometric features**, employing equivalent tools and following the pre-defined workflow. As a result, among ten attributes, seven were preserved: **Area, Perimeter, AtoP, PtoA, Shape, Compact and Fractal Index**.

Pondering that the quality of input attributes is the key for a successful prediction model, a deeper analysis was conducted to ascertain if the geometric and spectral features perform better isolated or in an integrated fashion. In this sense, adopting the features selected by the EDA as input, the next steps specified the best group of features and algorithms fitting parameters.

The software prototype made possible to perform all data combinations, amplifying the number of iterations to design global and specific models for 5 different scenarios. The same six ML algorithms were implemented and evaluated.

In general, the accuracies using only geometric features (71.46%, LR) were better than using only spectral (70.24%, DT). However, the integration between them improved the performances reaching 73.15% of maximum accuracy in RF, being the best-input option for the CM building.

The DT and NB had an inverse behavior for spectral and geometric attributes. It is noticeable that the DT and NB are the ones with the most unstable performances throughout the classifiers, returning the worst accuracies, with values below the average for almost all combinations of attributes. Consequently, they were not considered in the subsequent analysis. The ANN, LDA and LR returned the most stable performances, with similar behavior for all groups of features. Considering the geometric and spectral features integration, the RF and ANN returned the better performances for OSS discrimination.

Since the performance of the algorithms is case-specific, the next analysis used as input the 12 selected features keeping the parametric (LDA and LR) and nonparametric (ANN and RF) approaches. The goal is to find the proper inference method to derivate SCM from the global CM considering different seasons.

The available database indicates the season that each oil slick was detected, giving indirect clues about the wind behavior. This information allows to evaluate the benefits

of building and fitting SCM considering the seasonality effect, once the GoM presents significant variations in terms of wind intensity and direction across the year.

To accomplish this, five scenarios were investigated, as follows: (a) all seasons together (ALL); (b) Winter; (c) Spring; (d) Summer; (e) Fall. The maximum prediction accuracies obtained using the four ML algorithms are presented in Table 1(a), while the median accuracies are shown in Table 1(b).

Table 1 *– (a) Maximum accuracies and (b) median accuracies for all seasons together (ALL) and for each season, indicating the performance of the algorithms (RF, ANN, LDA and LR).*

(a) Maximum Accuracies					
	All	**Winter**	**Spring**	**Summer**	**Fall**
RF	**73.15**	**80.51**	**77.76**	**73.82**	72.93
ANN	73.02	77.98	75.15	72.65	73.48
LDA	72.07	78.34	75.35	72.94	73.20
LR	72.00	78.34	73.75	71.76	**75.14**

(b) Median Accuracies					
	All	**Winter**	**Spring**	**Summer**	**Fall**
RF	**71.53**	74.91	**75.80**	**70.80**	**68.65**
ANN	70.04	**75.45**	71.99	69.77	67.82
LDA	70.14	74.55	72.99	67.26	**68.79**
LR	70.24	75.27	71.39	67.11	68.51

Figure 2 provides the median accuracies for all tested ML algorithms plotting the average and maximum trends as reference.

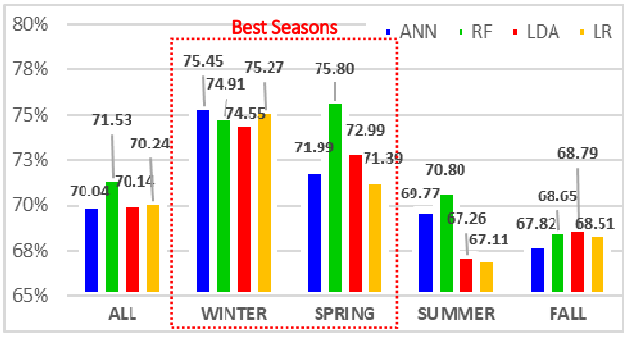

Figure 2 *– Comparison between median accuracies achieved by all tested ML algorithms.*

The higher accuracies are obtained during Winter (Max: 80.51; Median: 75.45) and Spring (Max: 77.76; Median: 75.80), while the worst predictions are observed during Summer (Max: 73.82; Median: 70.80) and Fall (Max: 75.14; Median: 68.79). The consistency of results was demonstrated by a historical database containing more than 100 years of hurricanes and tropical storms records (Figure 3). This database is provided by the National Oceanic and Atmospheric Administration (NOAA) [14] and shows that the months with the highest incidence of extreme weather events (August, September, and October) coincide with the worst seasons indicated by the prediction models (compare figures 2 and 3).

The occurrence of high-intensity winds during the Summer and Fall certainly contributed to the worst performance of these models to distinguish natural from anthropic oil slicks. Moreover, precisely during the years of the project's database development (2008-2012), the time-series of records evidenced a higher incidence of extreme weather events, notably with major hurricanes above the average, reinforcing the achieved results.

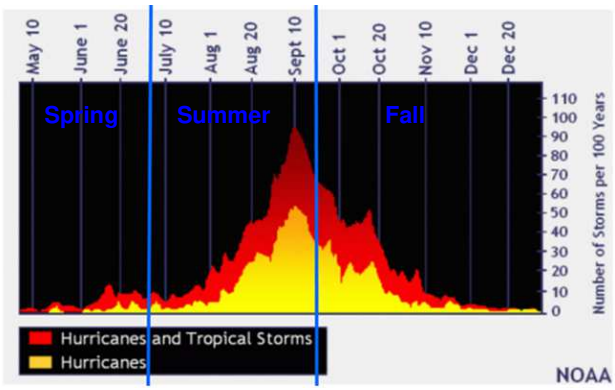

Figure 3 *– Number of hurricanes and tropical storms in the Atlantic (Atlantic Ocean, Caribbean Sea and Gulf of Mexico): 100-year historical series of data provided by NOAA. Source: https://www.nhc.noaa.gov/climo/.*

Regarding the ML algorithms, the RF returned the highest median accuracies for almost all seasons. It is interesting to note that the maximum accuracy achieved using the complete dataset (73.15%) is lower than the ones that correspond to the best (Winter: 80.51%) and the worst (Summer: 73.82%) seasonal scenarios.

The research results indicate that seasonality causes a significant impact over the OSS identification in the GoM. The best seasons to acquire SAR data to distinguish seeps from spills are Winter and Spring. The predictions obtained demonstrated the potential offered by the models' specification in terms of features, algorithms, and parameters selection.

Conclusions

The database dimensionality was successfully reduced from 418 to 12 features thought the EDA, preserving the representativeness of the data without compromising the classification accuracies. Regarding the seasonality, the best median accuracies are reached in Winter (75.45%) and Spring (75.80%), while the worst are found in Summer (70.80%) and Fall (68.79%). Consistently, the worst seasons coincide with the occurrence of hurricanes in the GoM, when high-intensity winds hamper oil slick detection using SAR instruments.

The RF was found to be the most robust ML method for distinguishing seeps from spills. The adopted approach

demonstrated that the proposed SCM is operational under different real-world conditions. The generalization capacity of the developed models will be assessed in future initiatives in the Brazilian Continental Margin. The contribution of new features and further ML algorithms to improve the OSS prediction will also be exploited.

Acknowledgments

The authors are grateful to Petróleo Brasileiro S.A. (Petrobras) for providing funds for this project. In addition, the authors would like to credit the Software Engineering Lab (LES), from Pontifical Catholic University from Rio de Janeiro (PUC-Rio), for providing all in-house software used to process the dataset.

References

[1] API: American Petroleum Institute (2013). "Remote sensing in support of oil spill response: Planning guidance," Amer. Petroleum Inst., Washington, DC, USA, API Tech. Rep. no. 1144, Sep. 2013.

[2] IPIECA: International Petroleum Industry Environmental Conservation Association (2014). "An assessment of surface surveillance capabilities for oil spill response using satellite remote sensing," International Petroleum Industry Environmental Conservation Association, London, U.K., Tech. Rep. PIL- 4000–35-TR-1.0, Jan. 2014.

[3] G. A. Carvalho, P. J. Minnett, E. T. Paes, F. P. Miranda, L. Landau (2019). Oil-Slick Category Discrimination (Seeps vs. Spills): A Linear Discriminant Analysis Using RADARSAT-2 Backscatter Coefficients (σ_0, β_0, and γ_0) in Campeche Bay (Gulf of Mexico). Remote Sens. 2019, 11, 1652; doi:10.3390/rs11141652

[4] C. Brekke and A. H. S. Solberg, "Oil spill detection by satellite remote sensing – Review," Remote Sens. Environ., vol. 95, no. 1, pp. 1–13, Mar 2005.

[5] M. J. Caruso, M. Migliaccio, J. T. Hargrove, O. Garcia-Pineda, and H. C. Graber (2013). "Oil spills and slicks imaged by synthetic aperture radar," Oceanography, vol. 26 no. 2, pp. 112–123, 2013. [Online]. Available: http://dx.doi.org/10.5670/oceanog.2013.34

[6] Werner Alpers, Benjamin Holt, Kan Zeng. Oil spill detection by imaging radars: Challenges and pitfalls. Remote Sensing of Environment, Volume 201, November 2017, Pages 133-147. http://dx.doi.org/10.1016/j.rse.2017.09.002

[7] G. A. Carvalho, P. J. Minnett, E. T. Paes, F. P. Miranda, L. Landau (2018). Refined Analysis of RADARSAT-2 Measurements to Discriminate Two Petrogenic Oil-Slick Categories: Seeps versus Spills. J. Mar. Sci. Eng., 6, 153; doi:10.3390/jmse6040153

[8] G. Carvalho, F. P. Miranda, P.Minnet (2017). "Exploratory Data Analysis of Synthetic Aperture Radar (SAR) Measurements to Distinguish the Sea Surface Expressions of Naturally-Occurring Oil Seeps from Human-Related Oil Spills in Campeche Bay (Gulf of Mexico)". ISPRS International Journal of Geo-Information, v. 6, n. 12, p. 379, 2017. Available: <http://www.mdpi.com/2220-9964/6/12/379>. DOI: 10.3390/ijgi6120379

[9] G. A. Carvalho, P. J. Minnett, F. P. Miranda, L. Landau, F. Moreira (2016). The Use of a RADARSAT-Derived Long-Term Dataset to Investigate the Sea Surface Expressions of Human-Related Oil Spills and Naturally Occurring Oil Seeps in Campeche Bay, Gulf of Mexico, Canadian Journal of Remote Sensing, 42:3, 307-321, DOI: 10.1080/07038992.2016.1173532

[10] David J. Lary, Amir H. Alavi, Amir H. Gandomi, Annette L. Walker. Machine learning in geosciences and remote sensing. Geoscience Frontiers 7 (2016) 3e10. http://dx.doi.org/10.1016/j.gsf.2015.07.003

[11] A.E. Maxwell, T. A. Warner & F. Fang (2018). "Implementation of machine-learning classification in remote sensing: an applied review". International Journal of Remote Sensing, 39:9, 2784-2817, DOI: 10.1080/01431161.2018.1433343

Kubat, M., Holte, C., & Matwin, S. (1998). Machine learni[12] ng for detection of oil spills in satellite Radar images. Machine Learning, 30 (2-3), 195–215.

[13] Fernando Pellon de Miranda, Arturo Mendoza Quintero Marmol, Enrico Campos Pedroso, Carlos Henrique Beisl, Pamela Welgan, and Luis Medrano Morales (2004)."Analysis of RADARSAT-1 data for offshore monitoring activities in the Cantarell Complex, Gulf of Mexico, using the unsupervised semivariogram textural classifier (USTC)." Can. J. Remote Sensing, Vol. 30, No. 3, pp. 424–436, 2004.

[14] Time series recorded between 1851 and 2014 with the number of hurricanes and subtropical cyclones over the Atlantic (Regions of influence: Atlantic Ocean, Caribbean Sea, and Gulf of Mexico). Dataset provided by the National Oceanic and Atmospheric Administration (NOAA), consolidated by the National Hurricane Center and Central Pacific Hurricane Center. Accessed in May 2020: https://www.nhc.noaa.gov/climo/

[15] J. Z. Hidalgo, R.R. Centeno, A.M. Jasso (2014). "The response of the Gulf of Mexico to wind and heat flux forcing: What has been learned in recent years?". Atmósfera 27(3), 317-334.

[16] Henderson, F M, and Lewis, A J. Principles and applications of imaging radar. Manual of remote sensing: Third edition, Volume 2. United States: N. p., 1998. Web.

[17] Stephen Marsland. Machine Learning: an Algorithmic Perspective. Chapman & Hall/CRC Machine Learning & Pattern Recognition Series. Second Edition, 2015 CRC Press is an imprint of Taylor & Francis Group. ISBN: International Standard Book Number-13: 978-1-4665-8333-7